Fitting Dark Matter

Student lecture by Anja Butter

January 30, 2017

1 Introduction

While observations of clusters and the latest precise measurements of the relic density by Planck leave no doubts concerning the existence of dark matter - and as a consequence physics beyond the Standard Model - the actual nature of dark matter continues to escape our current research programs. The LHC, Planck, Fermi, Xenon1t are only some of the many experiments that have been or are searching for physics beyond the Standard Model. In order to obtain the strongest constraints on a dark matter model, one has to combine the results from direct, indirect and collider searches in a global analysis. This means we take into account all kinds of data, event numbers distributions, observables, and exclusion limits. The common point to all inputs is that we have to treat the uncertainties associated to our data in a careful and consistent way. In these lecture notes we will first discuss the details of such a statistical analysis. For this purpose we will illustrate different types of uncertainties by means of the γ-ray spectrum obtained by Fermi-LAT. In the second chapter we will review the "WIMP" model, as a solution to the dark matter problem, and the associated calculation of the relic density and discuss typical annihilation channels using the example of supersymmetry. In the last chapter we will discuss a current paper on the galactic centre excess and the results of a global analysis, connecting direct, indirect, and collider searches.

2 Fitting

The basic idea of every fit is very simple. On the one hand we have data in form of event numbers or cross sections that have been measured by an experiment. On the other hand we have a model, that predicts the same observable. If data and prediction agree, the model is (for the time being) a valid description - if they do not agree, the model is excluded. Usually the model depends on a number of input parameters. A Markov chain can be used to search the parameter space for allowed regions or best fit points.
The complicated part is to define what we mean by "agree". We start with the

definition of probability as a frequentist concept. Let us assume we perform an experiment to measure the observable x. Repeating the experiment many times will result in different values of x. The resulting distribution generates the probability density function of x, $f(x)$. Using this distribution we can determine the probability p to measure x within the interval $[x_{min}, x_{max}]$

$$\int_{x_{min}}^{x_{max}} f(x)dx = p \tag{1}$$

This definition is well defined within the frequentist framework. In order to include our model we insert the dependence on a model parameter α and consider $f(x|\alpha)$. For each value of alpha the pdf is again normalised to 1.

$$\int_{-\infty}^{+\infty} f(x|\alpha)dx = 1 \tag{2}$$

Fixing x to an observed value, we define the likelihood function $\mathcal{L}(\alpha) = f(x|\alpha)$ that is no longer normalised to 1. Using the likelihood function one can determine the best fit value α_{best} for which the likelihood is maximal. For practical purpose one often minimises the log-likelihood $-2\log\mathcal{L}(\alpha)$ instead of maximising the likelihood as the product of likelihood becomes a simple sum of log-likelihoods. In the final analysis we will consider the likelihood ratio function, that divides the likelihood of a given parameter point by the likelihood of the best fit point. Under certain conditions this likelihood ratio function can be approximated by a χ^2 distribution, which finally allows us to perform actual hypothesis testing and exclude regions of the parameter space.
In the following we will discuss how to actually build a likelihood function.

2.1 How to build a likelihood function

The most crucial part when including data into a fit is the treatment of uncertainties. In order to build a correct likelihood function we have to assign the right shape - *Gaussian, Poisson, or flat* - to the different kinds of uncertainties - *systematic, statistic, theoretical* - and correlate them in the right way. In the following we will discuss the different kinds of uncertainties one by one. For illustration I will refer to the data from the Fermi-LAT (Large Area Telescope) publication [arXiv:1511.02938].

2.1.1 Fermi data

In the Fermi data, the main uncertainty comes from the determination of the background. Interactions of high energy cosmic rays with the interstellar gas and radiation field produce a diffuse γ- ray emission, which is the main background for a γ- ray spectrum from dark matter annihilation. Therefore the spatial distribution of cosmic rays sources is a crucial ingredient. In order to estimate the corresponding uncertainties, the Fermi-LAT collaboration uses two models, "OB-stars" and

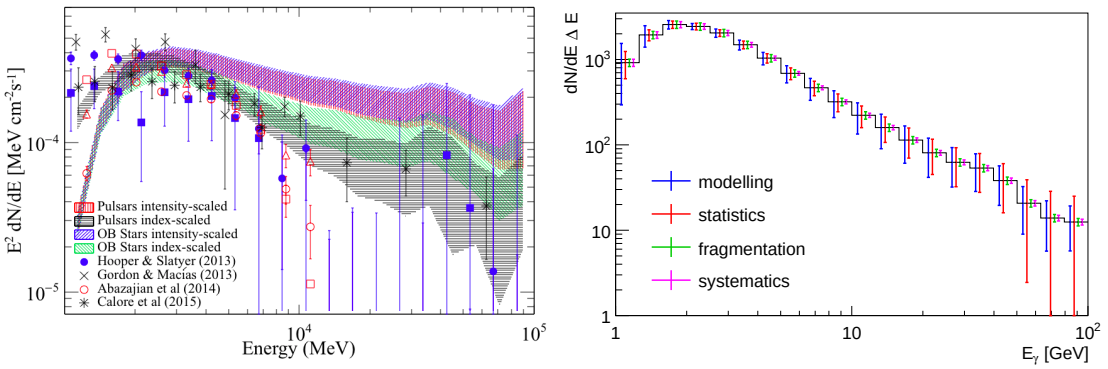

Figure 1: Left: Fermi spectrum as displayed in the publication by Fermi-LAT [arXiv:1511.02938]. Right: Spectrum averaged over the different backgrounds including all applied uncertainties.

"Pulsars" to model their distribution. Both models represent extreme cases. The pulsar distribution is non-zero around at the Galactic centre while the distribution of OB-stars vanishes around 2 kpc from the Galactic centre. For each model they apply two methods - index and intensity scaled - to model the background from interstellar emission. While for the intensity scaled case the normalisation of the used templates is the only free parameter, in the index scaled case, one allows the coefficient of the gas-related interstellar emission model to vary. Fig. 1 shows the background subtracted data for all four models. For an accurate fit of the spectrum we will include the entire spectrum bin by bin. We start by determining the individual likelihood contributions χ_i, which are then combined taken into account correlations of uncertainties.

2.1.2 Poisson distribution

The statistic uncertainty is inherent to every measurement. Poisson statistic can be applied to describe statistic uncertainties when we consider a large number of independent tries N, a small probability p to observe an event and when the product of probability and the number of tries results in a finite number of events $N \cdot p$. These conditions are exactly fulfilled at the LHC, as well as the observation of γ-rays from the galactic centre. The probability to observe d events when you expect $\tilde{d}$ events is then given by

$$\mathcal{L}_{Poiss,d} = P(d|\tilde{d}) = \frac{e^{-\tilde{d}}\tilde{d}^d}{d!} \tag{3}$$

This distribution peaks between $d = \tilde{d} - 1$ and $d = \tilde{d}$ and is normalized to 1.

$$\sum_{d=0}^{d=\infty} P(d|\tilde{d}) = e^{-\tilde{d}} \sum_{d=0}^{d=\text{inf}} \frac{\tilde{d}^d}{d!} = e^{-\tilde{d}} e^{\tilde{d}} = 1 \tag{4}$$

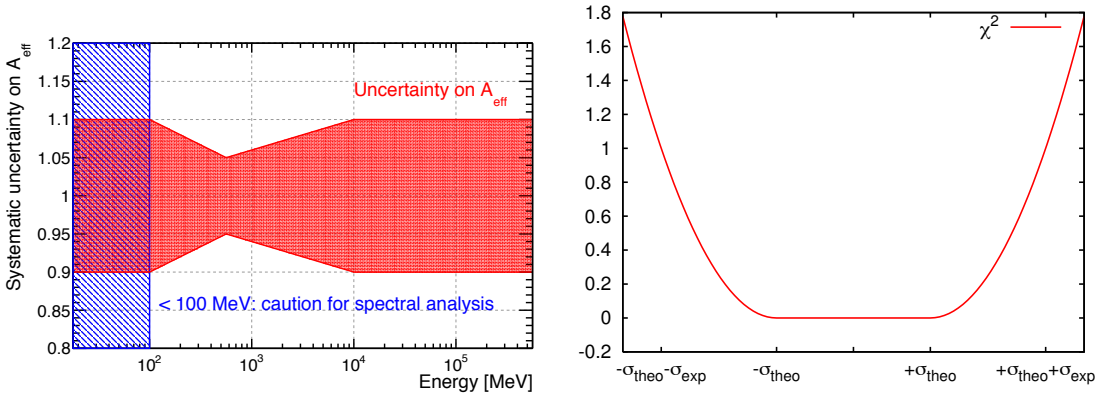

Figure 2: Left: Systematic uncertainty band on the effective area A_{eff} as a function of energy. [arXiv: 1206.1896]. Right: Illustration of the R-fit scheme for the combination of flat and Gaussian uncertainty.

We normalize the likelihood again such, that $\mathcal{L}(d = \tilde{d}) = 1$:

$$\mathcal{L}_{\text{Poiss},d} = \frac{P(d|\tilde{d})}{P(\tilde{d}|\tilde{d})} = \frac{\tilde{d}!}{d!}\,\tilde{d}^{d-\tilde{d}} \tag{5}$$

The statistical uncertainty on the background is independent from the uncertainty on the data or in other words: a deviation of predicted signal and measured signal can be caused by a fluctuation of the data as well as a fluctuation of the background. We take this into account by a second contribution to the likelihood that compares the measured background b with the predicted background $\tilde{b}$. For the measured background we take the numbers given by the paper. For the predicted background we add the difference between measured and predicted data $\tilde{b} = b + \tilde{d} - d$, assigning the full deviation to the background. The second contribution to the likelihood is therefore given by

$$\mathcal{L}_{\text{Poiss},b} = \frac{P(b|\tilde{b})}{P(\tilde{b}|\tilde{b})} = \frac{(b+\tilde{d}-d)!}{b!}\,(b+\tilde{d}-d)^{d-\tilde{d}}. \tag{6}$$

2.1.3 Gaussian distribution

Next we are going to discuss systematic uncertainties, that usually arise in the context of calibration of the experiment. Typical examples are the uncertainty on the luminosity of a collider or the photon reconstruction efficiency of a calorimeter for instance at Fermi-LAT or at an LHC experiment. Fig. 2 shows the systematic uncertainty on the effective detection surface A_{eff} of the Fermi-LAT. The effective area is the product of the cross-sectional geometrical collection area, the γ-ray conversion probability, and the efficiency of a given event selection for a γ-ray depending on its energy and direction in the LAT frame. Usually systematic uncertainties can

be described by a Gaussian distribution, since they are measured using large data samples. The likelihood is given by

$$\mathcal{L}_{Gauss}(d|\tilde{d}) = \frac{1}{\sqrt{2\sigma_{sys}^2\pi}} \exp - \frac{\left(d-\tilde{d}\right)^2}{2\sigma_{sys}^2} \tag{7}$$

where d stands for the actually measured data and $\tilde{d}$ for the predicted number of events. Moving from likelihood to log-likelihood, the pre-factor becomes a constant offset. We want to normalize the likelihood such, that $\mathcal{L}(d=\tilde{d})=1$.

$$-2\log\mathcal{L}_{Gauss}(d|\tilde{d}) = \frac{\left(d-\tilde{d}\right)^2}{\sigma_{sys}^2} = \chi^2 \tag{8}$$

When we are looking for physics beyond the Standard Model we consider the Standard Model as a background and the data as the sum of signal and background: $d = s + b$. What we are actually looking for is therefore the likelihood of the BSM signal $\tilde{s}$ given the datapoint $s = d - b$. The resulting uncertainty depends on the correlation of data and background:

$$\sigma_s^2 = \left(\frac{\partial s}{\partial d}\sigma_d\right)^2 + \left(\frac{\partial s}{\partial b}\sigma_b\right)^2 + 2\rho\frac{\partial s}{\partial d}\frac{\partial s}{\partial b}\sigma_d\sigma_b \tag{9}$$

$$= \begin{cases} \sigma_d^2 + \sigma_b^2 & \text{for } \rho = 0 \text{ (uncorrelated)} \\ (\sigma_d - \sigma_b)^2 & \text{for } \rho = 1 \text{ (fully correlated)} \end{cases} \tag{10}$$

ρ is the correlation coefficient that can vary between -1 and 1. As the background estimation has been verified using the same experiment, we assume full correlation between data and background. Including all information we can therefore express the log-likelihood of one bin including the systematic uncertainty via

$$-2\log\mathcal{L}_{Gauss}(s|\tilde{s}) = \frac{(d-b-\tilde{s})^2}{\sigma_{sys,s}^2}. \tag{11}$$

2.1.4 Flat distribution

The third class of uncertainties are described by a flat distribution.

$$\mathcal{L}_{\text{Flat},d} = \Theta(d - \tilde{d} + \sigma_{d,1})\Theta(\tilde{d} - d + \sigma_{d,2}) \tag{12}$$

In this case the prediction has to be within a certain range of the data, otherwise its likelihood vanishes. Within the allowed range there is no discrimination between the values. A typical situation in which we apply these kind of uncertainties are scale dependencies in higher order calculations. In this case this treatment has no statistical signification and the values of "σ" do NOT correspond to a well defined statistical interpretation. A common way to determine σ_d is e.g. to vary the scale

that is used in the calculation of the observables by a factor of 2 in both directions. In the case of the Fermi spectrum we use a flat uncertainty to cover the differences between the different background models. As we have no means to determine which model is closer to a "true" model, we have to assume that the likelihood distribution is flat between the minimal and maximal value predicted by the model.

2.2 Combination

Having determined the forms of all uncertainties, we proceed to combine them into one likelihood function. In order to combine e.g. theory and systematic uncertainty we profile over the theory uncertainty. This results in a shift of the predicted data towards the actual data

$$\mathcal{L} = \max_{s^*} \Theta\left[s^* - (\tilde{s} - \sigma_{theo})\right] \Theta\left[(\tilde{s} + \sigma_{theo}) - s^*\right] \exp - \frac{\left(d - b - s^*\right)^2}{2\sigma_{sys,s}^2} \tag{13}$$

$$= \max_{s^*[\tilde{s}_{min}, \tilde{s}_{max}]} \exp - \frac{\left(d - b - s^*\right)^2}{2\sigma_{sys,s}^2}. \tag{14}$$

The log-likelihood can therefore be expressed by

$$\sqrt{-2\log\mathcal{L}} = \chi = \begin{cases} \dfrac{s - (\tilde{s} + \sigma_{theo})}{\sigma_{sys,s}} & \text{for } \sigma_{theo} < s - \tilde{s} \\ 0 & \text{for } \sigma_{theo} > |s - \tilde{s}| \\ \dfrac{s - (\tilde{s} - \sigma_{theo})}{\sigma_{sys,s}} & \text{for } \sigma_{theo} < \tilde{s} - s \end{cases} \tag{15}$$

The combination of theory and statistic uncertainty follows the same approach and results again in a shift of the prediction towards the data. The combination of Poisson and Gauss distributions usually needs a numerical solution. However we found that the approximative formula

$$\frac{1}{\log\mathcal{L}} = \frac{1}{\log\mathcal{L}_{Gauss}} + \frac{1}{\log\mathcal{L}_{Poiss,d}} + \frac{1}{\log\mathcal{L}_{Poiss,b}} \tag{16}$$

that is valid in the limit of large event numbers, results as well in a very good agreement for small event numbers, reducing the computing time. The expression illustrates that the combined likelihood is dominated by the largest likelihood, which corresponds to the largest uncertainty.

2.3 Correlations

We already mentioned the necessity of including correlations between the data and the background. When combining the likelihood contributions of all bins we have to take into account as well the correlation of systematic uncertainties of the same type between different bins. This can be implemented using a correlation matrix

$$C_{i,j} = \frac{\sum_{syst} \sigma_{i,syst}\sigma_{j,syst} \cdot \mathrm{corr}(i,j)}{\sigma_{i,exp}\sigma_{j,exp}}, \tag{17}$$

where we sum over all systematic uncertainties. $\sigma^2_{i,exp}$ is the sum of all experimental - non theoretical - uncertainties added in quadrature. The full log-likelihood is finally computed using:

$$\chi^2 = \vec{\chi_i}^T C^{-1} \vec{\chi_i} \tag{18}$$

Theoretical uncertainties are not included in the above calculation. In the case of Fermi we assume that they are uncorrelated, as all models use a legitimate approach and the correlations would depend on the specific models. Correlated theory uncertainties can be modelled using nuisance parameters, that can vary within a certain interval corresponding to σ_{theo}. The global fit then profiles over this parameter.

3 Dark Matter

3.1 Evidence for dark matter

The first evidences for dark matter were observed and pointed out by Jan Hendrik Oort and Fritz Zwicky in 1932 and 1933. While Oort's measurement was later found to be incorrect, Zwicky's observations were determined from observations of the Coma galaxy cluster. Using the virial theorem he estimated its mass from the movement of galaxies at the outer part of the cluster. From the comparison with the brightness and number of galaxies he deduced a factor of 400 between the visible and the dark matter. The number was later corrected to be smaller by an order of magnitude e.g. due to updated values of the Hubble constant. In the following years many other observations have supported this theory. Typical examples are

- Galaxy rotation curves
- Dynamics of galaxy clusters
- Cosmic microwave background (CMB)
- Collisions of galaxy clusters
- Structure Formation.

All evidence can be explained by weakly interacting massive particles (WIMPs). As the name suggests they are not charged under the electromagnetic force but interact only weakly. Recent measurements of the CMB by Planck have determined the relic density with high precision. We will now calculate how to predict the relic density from the annihilation cross section of a WIMP particle.

3.2 The WIMP relic density

Following modern models of the Big Bang the history of the early universe is a rather short one. This is not to say, that nothing happened - quite the contrary - but about half of the crucial steps are assumed to happen within the first few minutes. There is inflation at about 10^{-34} s after the Big Bang, followed closely by baryogenesis and electroweak phase transition at $2 \cdot 10^{-11}$ s. As the temperature continues to drop the QCD phase transition takes place after $2 \cdot 10^{-5}$ s. This is roughly the same time when we expect the dark matter to freeze out. In the following couple of minutes we can see the neutrinos decouple (1 s), electrons and positrons annihilate (6 s), and finally the nucleosynthesis forming light elements. The following processes of recombination will take several thousands of years ending with the decoupling of photons that we can observe today as the cosmic microwave background. The formation of stars and galaxies seems in comparison only a minor step that will be neglect in the following discussion ;).
When we talk about the freeze out of dark matter, which determines the relic density,

we have to go back to the first microseconds after the Big Bang. In the time after the inflation dark matter was in thermal equilibrium.

$$\frac{dN_\chi}{dt} = 0 \tag{19}$$

The equilibrium is described by the Boltzmann equation, where any change in the number of dark matter particles comes from annihilation of dark matter into SM particles and vice versa.

$$\frac{dN_\chi}{dt} = \Gamma(f\bar{f} \to \chi\chi) - \Gamma(\chi\chi \to f\bar{f}) + \Gamma_{other} \tag{20}$$

We can directly see that when the temperature drops below the mass of the dark matter particle, only SM particles at the tail of the velocity distribution could produce dark matter particles, while the dark matter particles can annihilate into SM particles and thereby decrease N_χ. Only when due to the expansion of the universe the number density of dark matter has dropped sufficiently that the probability of one DM particle to find another is small, N_χ will become constant again. This process is called freeze-out and we will go through the main step of the calculation to determine the relic density.
Starting with the left hand side of eq. (20) we have to take into account the expansion of the universe. A change of the number of dark matter particles can either be related to a change in the number density or in the volume.

$$\frac{dN_\chi}{dt} = \frac{d(n_\chi V)}{dt} = V\frac{dn_\chi}{dt} + 3n_\chi HV \quad \text{with} \quad H(t) = \frac{\dot{a}(t)}{a(t)} \tag{21}$$

The Hubble constant quantifies the expansion of the universe. The transition rates on the right hand side of the Boltzmann equation can be calculated via

$$\begin{aligned}\Gamma(\chi_1\chi_2 \to f_1\bar{f}_2) =& V\int d\Pi(p_1)d\Pi(p_2)d\Pi(k_1)d\Pi(k_2)\phi_{\chi_1}\phi_{\chi_2}(1\pm\phi_{f_1})(1\pm\phi_{f_2}) \\ & (2\pi)^4\delta^{(4)}(p_1+p_2-k_1-k_2)\overline{|\mathcal{M}_{\chi_{k_1}\chi_{k_2}\to f_{p_1}\bar{f}_{p_2}}|}^2\end{aligned} \tag{22}$$

where ϕ is the phase space density of the involved particles. The plus corresponds to bosonic final states and the minus to fermionic final states. $\overline{|\mathcal{M}|}$ is the spin averaged matrix element. Assuming CP invariance we can use that

$$|\mathcal{M}_{\chi_{k_1}\chi_{k_2}\to f_{p_1}\bar{f}_{p_2}}|^2 = |\mathcal{M}_{f_{p_1}\bar{f}_{p_2}\to\chi_{k_1}\chi_{k_2}}|^2 = |\mathcal{M}|^2. \tag{23}$$

Moreover we use Maxwell-Boltzmann statistics for all involved particles leading to $\phi_i(k_i) = \exp[-(E_i-\mu_i)/T]$ in equilibrium with a negligible chemical potential μ_i and $1\pm\phi_i \approx 1$. The full Boltzmann equation then simplifies to

$$\begin{aligned}\frac{dn_\chi}{dt} + 3n_\chi H =& \int d\Pi(p_1)d\Pi(p_2)d\Pi(k_1)d\Pi(k_2)(\phi_{f_1}\phi_{f_2}-\phi_{\chi_1}\phi_{\chi_2}) \\ & (2\pi)^4\delta^{(4)}(p_1+p_2-k_1-k_2)\overline{|\mathcal{M}|}^2.\end{aligned} \tag{24}$$

The δ function enforces $E_{\chi_1} + E_{\chi_2} = E_{f_1} + E_{\bar{f}_2}$ and we can express the phase space density of the SM particle via

$$\begin{aligned}\phi_{f_1}\phi_{f_2} = \phi_{f_1,eq}\phi_{f_2,eq} &= \exp[-(E_{f_1} + E_{\bar{f}_2})/T] \\ &= \exp[-(E_{\chi_1} + E_{\chi_2})/T] = \phi_{\chi_1,eq}\phi_{\chi_2,eq}. \end{aligned} \tag{25}$$

The first equality arises because the SM particle will remain in thermal equilibrium during the freeze out due to its interactions with the SM sector. The next step is to connect the decay rate with the annihilation cross section. The thermal average of the cross section times the relative velocity of the annihilating particles is

$$\begin{aligned}< \sigma_{ann} v_{rel} > = &\frac{1}{n_\chi} \int d\Pi(p_1) d\Pi(p_2) d\Pi(k_1) d\Pi(k_2) (\phi_{f_1}\phi_{f_2} - \phi_{\chi_1}\phi_{\chi_2}) \\ &(2\pi)^4 \delta^{(4)}(p_1 + p_2 - k_1 - k_2) \overline{|\mathcal{M}|}^2. \end{aligned} \tag{26}$$

Inserting this expression into the Boltzmann equation we obtain

$$\frac{dn_\chi}{dt} + 3n_\chi H = - < \sigma_{ann} v_{rel} > (n_\chi^2 - n_{\chi,eq}^2). \tag{27}$$

Before we can solve the differential equation we will use two useful replacements. First we define

$$Y = \frac{n}{s} \qquad \text{with } \frac{dY}{dt} = \frac{1}{s}\frac{dn}{dt} + \frac{3}{R}\frac{dR}{dt} Y. \tag{28}$$

Here s is the entropy density. We use that the expansion is adiabatic, so that the entropy is conserved $sR^3 = const$. This leads to the first simplification

$$\frac{dY}{dt} = - < \sigma_{ann} v_{rel} > s(Y^2 - Y_{eq}^2). \tag{29}$$

The second simplification is to replace the time derivative by the temperature via

$$x = \frac{m_\chi}{T} \qquad \text{with } \frac{dY}{dt} = \frac{dY}{dx}\frac{H(m)}{x}. \tag{30}$$

The final form of our equation is

$$\frac{dY}{dx} = - < \sigma_{ann} v_{rel} > \frac{xs}{H(m)} (Y^2 - Y_{eq}^2). \tag{31}$$

We now that around the freeze out the equilibrium distribution drops exponentially and can therefore be neglected. We can now integrate out

$$\int_{Y(x_f)}^{Y(\infty)} \frac{1}{Y^2} dY = - < \sigma_{ann} v_{rel} > \frac{1}{H(m)} \int x s dx \tag{32}$$

$$-\frac{1}{Y(\infty)} = - < \sigma_{ann} v_{rel} > const \tag{33}$$

$$Y(\infty) = \frac{const}{< \sigma_{ann} v_{rel} >} \tag{34}$$

$$\Omega h^2 = \frac{\rho}{\rho_{crit}} h^2 = \frac{m_\chi Y(\infty) s}{\rho_{crit}} h^2 = \frac{const}{< \sigma_{ann} v >} \approx \frac{2.510^{-27} \frac{cm^3}{sec}}{< \sigma_{ann} v_{rel} >} \tag{35}$$

	SM Particle (R=+1)			SUSY Partner(R=-1)		
Names	Gauge ES	Mass ES	Spin	Gauge ES	Mass ES	Spin
squarks	$u_{L/R}, c_{L/R}, t_{L/R}$	u, c, t	1/2	$\tilde{u}_{L/R}, \tilde{c}_{L/R}, \tilde{t}_{L/R}$	$\tilde{u}_{1/2}, \tilde{c}_{1/2}, \tilde{t}_{1/2}$	0
	$d_{L/R}, s_{L/R}, b_{L/R}$	d, s, b	1/2	$\tilde{d}_{L/R}, \tilde{s}_{L/R}, \tilde{b}_{L/R}$	$\tilde{d}_{1/2}, \tilde{s}_{1/2}, \tilde{b}_{1/2}$	0
sleptons	$e_{L/R}, \mu_{L/R}, \tau_{L/R}$	e, μ, τ	1/2	$\tilde{e}_{L/R}, \tilde{\mu}_{L/R}, \tilde{\tau}_{L/R}$	$\tilde{e}_{1/2}, \tilde{\mu}_{1/2}, \tilde{\tau}_{1/2}$	0
	ν_e, ν_μ, ν_τ	ν_e, ν_μ, ν_τ	1/2	$\tilde{\nu}_e, \tilde{\nu}_\mu, \tilde{\nu}_\tau$	$\tilde{\nu}_e, \tilde{\nu}_\mu, \tilde{\nu}_\tau$	0
neutralinos	W^0, B^0	Z^0, γ	1	$\tilde{W}^0, \tilde{B}^0$	$\tilde{\chi}_1^0, \tilde{\chi}_2^0, \tilde{\chi}_3^0, \tilde{\chi}_4^0$	1/2
	H_u^0, H_d^0	h_1^0, h_2^0, A_1^0	0	$\tilde{H}_u^0, \tilde{H}_d^0$		
charginos	$W^\pm$	$W^\pm$	1	$\tilde{W}^\pm$	$\tilde{\chi}_1^\pm, \tilde{\chi}_2^\pm$	1/2
	H_u^+, H_d^-	$H^\pm$	0	$\tilde{H}_u^+, \tilde{H}_d^-$		
gluino	g	g	1	$\tilde{g}$	$\tilde{g}$	1/2

Table 1: Overview of SM particles and their supersymmetric partners in the MSSM

3.3 SUSY - a model for dark matter

Supersymmetry (SUSY) is one of the most popular models that predict physics beyond the SM, as it offers a solution to the Hierarchy problem and a dark matter candidate. Via an extension of the Poincaré algebra SUSY adds a symmetry to the SM that relates fermions and bosons, as listed in Tab. 1. It illustrates the full particle content of the minimal supersymmetric extension of the SM (MSSM) that leaves us with 31 undetected particles. If the symmetry was unbroken we would expect to observe the supersymmetric particles at the same masses as their SM partners. As these particles have not yet been observed, supersymmetry has to be broken. This forces us to introduce a soft SUSY breaking Lagrangian that leaves the coupling unchanged but can push the masses of charged particles to higher values and finally out of the so far detectable mass range. A general Ansatz for this Lagrangian is

$$\begin{aligned} L_{soft}^{MSSM} = & - \tilde{Q}^\dagger \mathbf{m_Q^2} \tilde{Q} - \tilde{L}^\dagger \mathbf{m_L^2} \tilde{L} - \tilde{\bar{u}}^\dagger \mathbf{m_{\bar{u}}^2} \tilde{\bar{u}}^\dagger - \tilde{\bar{d}}^\dagger \mathbf{m_{\bar{d}}^2} \tilde{\bar{d}}^\dagger - \tilde{\bar{e}}^\dagger \mathbf{m_{\bar{e}}^2} \tilde{\bar{e}}^\dagger \\ & - m_{H_u}^2 H_u^* H_u - m_{H_d}^2 H_d^* H_d - (m_3^2 H_u H_d + c.c.) \\ & - (\tilde{\bar{u}} \mathbf{h_u A_u} \tilde{Q} H_u + \tilde{\bar{d}} \mathbf{h_d A_d} \tilde{Q} H_d + \tilde{\bar{e}} \mathbf{h_e A_e} \tilde{L} H_d + c.c.) \\ & - \frac{1}{2}(M_3 \tilde{g}\tilde{g} + M_2 \tilde{W}\tilde{W} + M_1 \tilde{B}\tilde{B} + c.c.). \end{aligned} \tag{36}$$

For our purpose of explaining the relic density we are interested in the MSSM dark matter candidate. If R-parity, a Z_2 symmetry that protects baryon and lepton number conservation, was conserved, the lightest supersymmetric particle would be stable (LSP). If the LSP was in addition electromagnetically neutral, it would provide a good dark matter candidate. Valid solutions are neutralinos, sneutrinos or possibly a gravitino, that is not included in our model. A standard sneutrino solution is excluded due to the required annihilation cross section. The minimal required cross section would have led to discovery via Z-boson interactions. The only possibility to find sneutrino solutions is by including sterile sneutrinos. The

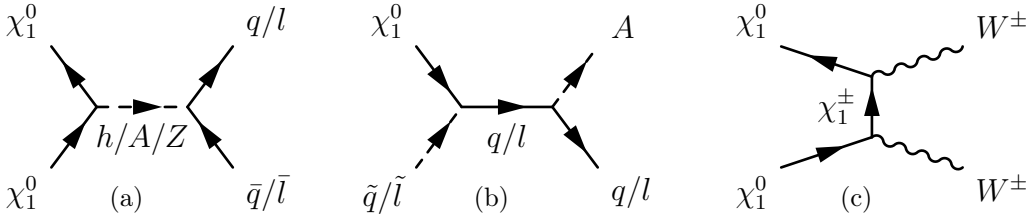

Figure 3: Dark matter annihilation processes for the funnel region (a), the co-annihilation region (b) and the focus point (c).

more popular solution is therefore neutralino dark matter. Its mass is determined by the neutralino mass mixing matrix

$$M_\chi = \begin{pmatrix} M_1 & 0 & -m_Z c_\beta s_w & m_Z s_\beta s_w \\ 0 & M_2 & m_Z c_\beta c_w & -m_Z s_\beta c_w \\ -m_Z c_\beta s_w & m_Z c_\beta c_w & 0 & -\mu \\ m_Z s_\beta s_w & -m_Z s_\beta c_w & -\mu & 0 \end{pmatrix}. \tag{37}$$

For small M_1 the LSP is bino like, for small M_2 it becomes a wino and for small μ it becomes a higgsino mixture. The composition of the neutralino is important for its coupling to the gauge bosons and Higgs scalars.

$$g_{W\chi_1^\pm\chi_1^0} = \frac{g\sin\theta_w}{\cos\theta_w}\left(\frac{1}{\sqrt{2}}N_{14}V_{12}^* - N_{12}V_{11}^*\right) \tag{38}$$

$$g_{Z\chi_1^0\chi_1^0} = \frac{g}{2\cos\theta_w}\left(N_{13}N_{13} - N_{14}N_{14}\right) \tag{39}$$

$$g_{h\chi_1^0\chi_1^0} = \left(gN_{11} - g'N_{12}\right)\left(\sin\alpha\ N_{13} + \cos\alpha\ N_{14}\right) \tag{40}$$

$$g_{A\chi_1^0\chi_1^0} = \left(gN_{11} - g'N_{12}\right)\left(\sin\beta\ N_{13} - \cos\beta\ N_{14}\right) \tag{41}$$

We see that apart from the W-coupling all couplings rely on a Higgsino component of the LSP. Therefore smaller values of μ will usually lead to larger couplings. On the other hand μ always has to remain larger than 103 GeV because otherwise the mass of the lightest chargino can be less than 103 GeV and would be excluded by LEP searches. Putting the information on the masses and couplings together we can analyse some typical annihilation channels.

3.3.1 Annihilation channels

Following our calculation in section 3.2 we can estimate the relic density by computing the annihilation cross section. The main annihilation channels can be sorted into the categories s-channel, t-channel and co-annihilation as illustrated in Fig. 3.

s-channel

The simplest annihilation channel is the s-channel annihilation. Two dark matter particles annihilate via a boson ($h/H/A/Z/\gamma$) into SM particles. If the propagator

process	channel	σv
$\chi\chi \to A \to q\bar{q}$	s-channel	$\frac{3\lambda_{\chi A}^2 \lambda_{qA}^2}{2\pi} \frac{m_\chi^2}{(M_A^2 - 4m_\chi^2)^2}$
$\chi\chi \to h \to q\bar{q}$	s-channel	$\frac{3\lambda_{\chi h}^2 \lambda_{qh}^2}{8\pi} \frac{v^2 m_\chi^2}{(M_h^2 - 4m_\chi^2)^2}$
$\chi\chi \to Z \to q\bar{q}$	s-channel	$\frac{3\lambda_{\chi Z_{ax}}^2}{2\pi} \left[\frac{\lambda_{qZ_{ax}}^2 m_q^2}{M_Z^4} + \frac{v^2(\lambda_{qZ_{ax}}^2 + \lambda_{qZ_v}^2) m_\chi^2}{3(M_Z^2 - 4m_\chi^2)^2} \right]$
$\chi\chi \to \chi\tilde{q}\bar{q} \to q\bar{q}$	t-channel	$\frac{3\lambda_{\chi q\tilde{q}}^4 (m_q + m_\chi)^2}{8\pi (M_{\tilde{q}}^2 - m_q^2 + m_\chi^2)^2}$

Table 2: Some examples for simplified annihilation cross sections expanded in powers of v^2 assuming Majorana dark matter and light final states.

can be on-shell, the annihilation cross section becomes very large and is constrained by the width of the propagator. In table 2 we display the annihilation cross section multiplied by the relative velocity of the colliding particles for specific channels. The results are expanded in powers of v^2 and assume Majorana dark matter and light quarks as final states so that $m_q \ll m_\chi$. We see that the annihilation via a scalar is s-wave suppressed with respect to the pseudoscalar annihilation. For the Z boson only the axial vector component couples to the Majorana particles. The v-independent contribution is hence suppressed by the mass of the outgoing particles. Close to the on shell conditioin the v^2 suppressed term will therefore be dominant.

co-annihilation
If the mass difference between LSP and the next heavier particle is small, the decay of the heavier particle is suppressed and it can contribute to the annihilation of dark matter. Typical examples are stau, stop or chargino co-annihilation. The corresponding mediator particles are tau, top and the charged Higgs and W bosons.

t-channel
Two dark matter particles can as well annihilate via a super symmetric mediator like a neutralino, a chargino, or a sfermion in the t-channel. In principle we can again enhance the cross section by choosing masses that allow for an on shell propagator. However the additional freedom from the momentum fraction that propagates through the mediator washes out the effect.

Concluding remark on annihilation in the early universe and today
When we talk about the relic density we have to take into account the the higher temperature and therefore the larger velocity of dark matter in the early universe. Comparing annihilation cross sections depending on the dark matter mass in the early universe and today will therefore result in a broader distribution for the early universe. Fig. 4 shows relic density and annihilation cross section today for a h and

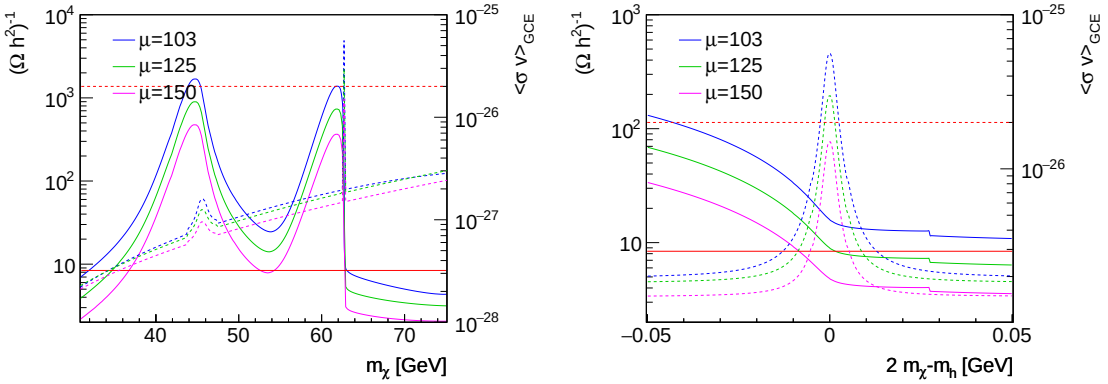

Figure 4: Inverse relic density (dashed, left axis) and annihilation rate in the GC (solid, right axis) for an MSSM parameter point where the annihilation is dominated by $\chi_1^0\chi_1^0 \to b\bar{b}$. The right pannel is zoomed into the Higgs annihilation region.

Z mediated annihilation. While the width in the relic density is determined by the velocity distribution, the width in the annihilation cross section today is determined by the width of the mediator.